APPLICATION NOTE

Multiskan Sky Microplate Spectrophotometer
and EVOS FL Auto Imaging System

Orthogonal approaches for studying bacterial biofilms using photometric detection with a Multiskan Sky Microplate Spectrophotometer and brightfield imaging with an EVOS FL Auto Imaging System

Inés Reigada,[1] Ilkka Miettinen,[2] Kirsi Savijoki,[3]
Adyary Fallarero[4]

[1,2,3] Anti-infective Research (AIR), Pharmaceutical Design and Discovery group (PharmDD), Faculty of Pharmacy, University of Helsinki, Finland

[4] Protein and Cell Analysis, Division of Biosciences, Thermo Fisher Scientific, Vantaa, Finland

Goal

This application note aims to demonstrate the benefits of using orthogonal approaches for studying *Staphylococcus aureus* biofilms—in particular, their susceptibility to antimicrobial agents. This is exemplified by performing a single adherence assay based on crystal violet staining, which allows both quantification of biofilm biomass and imaging of the attached cells. In the workflow presented here, the measurement of the photometric signal from the biomass-bound crystal violet dye was performed with a Thermo Scientific™ Multiskan™ Sky Microplate Spectrophotometer, which was complemented with the brightfield imaging of the microbial attachment pattern using an Invitrogen™ EVOS™ FL Auto Imaging System.

Introduction

Biofilms represent a complex multicellular sessile life-form of bacteria. These communities are formed embedded in a self-produced matrix, and they are considered responsible for a majority of antibiotic-tolerant infections [1]. Even in the case of biofilms formed by a single species, they are known to be inherently heterogeneous, which is related to both physiological and genetic factors. In the first case, chemical gradients give rise to different microenvironments within the biofilm where cellular populations with different metabolic rates coexist. In the second case, cells within the community may develop mutations that alter cellular responses and metabolic pathways. Thus, from a methodological perspective, addressing biofilm complexity is crucial, and it has become clear that a single endpoint is not enough to capture both the physical and functional complexities associated with biofilms [2]. Indeed, the use of a multiplicity of parameters, also known as orthogonal approaches, has proven to be a valuable strategy for achieving a deeper understanding of complex cellular events, such as those occurring in microbial biofilms [3].

Different endpoints have been successfully applied to biofilm analysis, focused on measuring bacterial viability (i.e., metabolic activity or membrane integrity) [4], quantifying the biofilm matrix [5], or estimating the biofilm biomass [6]. These quantitative methods are fast and technically easy to use [7], but they do not provide information on the spatial distribution of biofilms. Such information, typically obtained by imaging, is essential for revealing clues on cellular localization and heterogeneity within the biofilms. Techniques such as brightfield or fluorescence microscopy [8,9] combined with confocal laser scanning microscopy (CLSM) [10], fluorescence *in situ* hybridization (FISH) [11], and atomic force microscopy [12] have all been applied to biofilm imaging.

Crystal violet staining is widely used due to its low cost, simplicity, and compatibility with high-throughput screening [7]. It is particularly suited for genetic and antimicrobial screens, as well as for screening of biofilm formation on an abiotic surface under multiple growth conditions. Hydrophilic polystyrene has been the most frequently used surface in standard biofilm assays. Using this static biofilm system, nonadherent planktonic cells are removed and the biofilm cells that remain adhered to the surface are stained to allow visualization of the microbial attachment pattern. The dye bound to the biofilm biomass can also be further solubilized for a colorimetric quantitative assessment of the formed biofilms [13].

In this application note, a study of *Staphylococcus aureus* biofilms formed on polystyrene 96-well microtiter microplates with and without a model antibiotic, penicillin G, is reported. The benefits of combining different outcomes within a single staining assay were explored with the ultimate goal of understanding antimicrobial susceptibility of staphylococcal biofilms.

Materials and methods

Instruments

- Multiskan Sky Microplate Spectrophotometer
- EVOS FL Auto Imaging System
- Shaking incubator S1500 (Stuart)

Bacterial strains, reagents, and materials

- *Staphylococcus aureus* (ATCC, Cat. No. 25923)
- Tryptone Soy Broth, TSB (Lab M, Cat. No. LAB004)
- Tryptone Soy Agar, TSA (Lab M, Cat. No. LAB011)
- Thermo Scientific™ Nunc™ MicroWell™ 96-Well Microplates, Nunclon™ Delta surface (Thermo Fisher Scientific, Cat. No. 161093)
- Crystal violet solution (Sigma-Aldrich, Cat. No. HT90132-12)
- Phosphate-Buffered Saline, PBS (Lonza, Cat. No. BE17-516F)
- Penicillin G sodium salt (Sigma-Aldrich, Cat. No. 13752-5G-F)

Experiments

A pre-culture of *S. aureus* was prepared by adding 10 µL of the pure culture (maintained as a glycerol stock at –80°C) to 3 mL TSB, and the cells were cultured for 18 hr at 37°C under aerobic conditions (220 rpm). A 1:1,000 dilution of this pre-culture was made. This suspension was incubated (37°C, 220 rpm) for 4 hr, until the bacteria reached the exponential phase of growth (A_{595} = 0.38 ±0.01). Cell samples withdrawn at this growth stage were serially diluted and plated on TSA to determine the viable counts of bacteria (colony forming units, CFUs) after overnight incubation at 37°C.

To form biofilms, the exponentially grown cultures (10^6 CFU/mL) were added to Nunc 96-well microplates. Cells were exposed to either culture medium (untreated controls) or penicillin G (dissolved in PBS). To assess the effect of penicillin G in preventing biofilm formation (pre-exposure trials), 4 µL of penicillin G solution was added at the same time as the bacterial cultures (196 µL), and the plates were incubated at 37°C, 220 rpm for 18 hr. To assess the effect of penicillin G in the preformed biofilms (post-exposure trials), biofilms were first formed by adding planktonic bacterial suspensions to the plates (200 µL) and incubating the plates at 37°C under aerobic conditions (220 rpm) for 18 hr. Afterwards, the planktonic phase was removed and 4 µL of penicillin G solution was added along with the culture medium (196 µL). Plates were then returned to incubation conditions for an additional 18 hr at 37ºC. Final concentrations of penicillin G in the two exposure conditions were 0.1, 0.05, and 0.025 µM. In both conditions, wells containing only culture medium with PBS were included as negative controls.

To perform the crystal violet staining, the planktonic suspensions were removed from the plates at the end of the incubation periods, and the biofilms were fixed with 99.8% methanol (MeOH) (200 µL per well) for 15 min. After removal of MeOH, the wells were allowed to dry. Then 190 µL of crystal violet solution (0.0023%, v/v) was added and the cells were stained for 5 min at room temperature (RT), followed by two cycles of washing (200 µL per well) with Milli-Q™ water. Wells were allowed to dry for 15 min at RT. Next, brightfield images of the biofilms were captured using the EVOS FL Auto Imaging System (10x objective). Once pictures were taken, the crystal violet stain–bound biofilm was solubilized in 96% ethanol (200 µL per well). After 1 hr incubation at RT, the stained biofilm cells were quantitated by recording the absorbance at 595 nm using the Multiskan Sky Microplate Spectrophotometer (Figure 1).

Results and discussion

The formation of *S. aureus* biofilm biomass was quantitatively measured using crystal violet staining. As expected, the highest absorbance values were obtained in the untreated biofilms grown for 18 hr or 36 hr (A_{595} = 1.213 ±0.233 and 1.564 ±0.289, respectively), as opposed to the corresponding media controls (A_{595} = 0.156 ±0.019 and 0.148 ±0.014, respectively). The lowest and highest absorbance values within the plate can be quickly and easily identified with the aid of the user interface of the Multiskan Sky Microplate Spectrophotometer. Results of an assay can be viewed as numerical data or with a wavelength-adjusted heat map. Regardless of the selected view, the wells with the lowest and highest absorbance values are automatically identified and shown (Figure 2). Since it is wavelength-adjusted, an advantage of using the heat map view is that the color on the screen mimics the one seen in the actual test plate (in this case, the purple-blue color of the crystal violet stain). Actual variations within the crystal violet–bound biomass in the untreated biofilm wells are seen as different hues of blue in the user interface. This proprietary wavelength-adjusted heat map also allows quick identification of effective antibacterial treatments, and it further simplifies the identification of possible outliers within a plate.

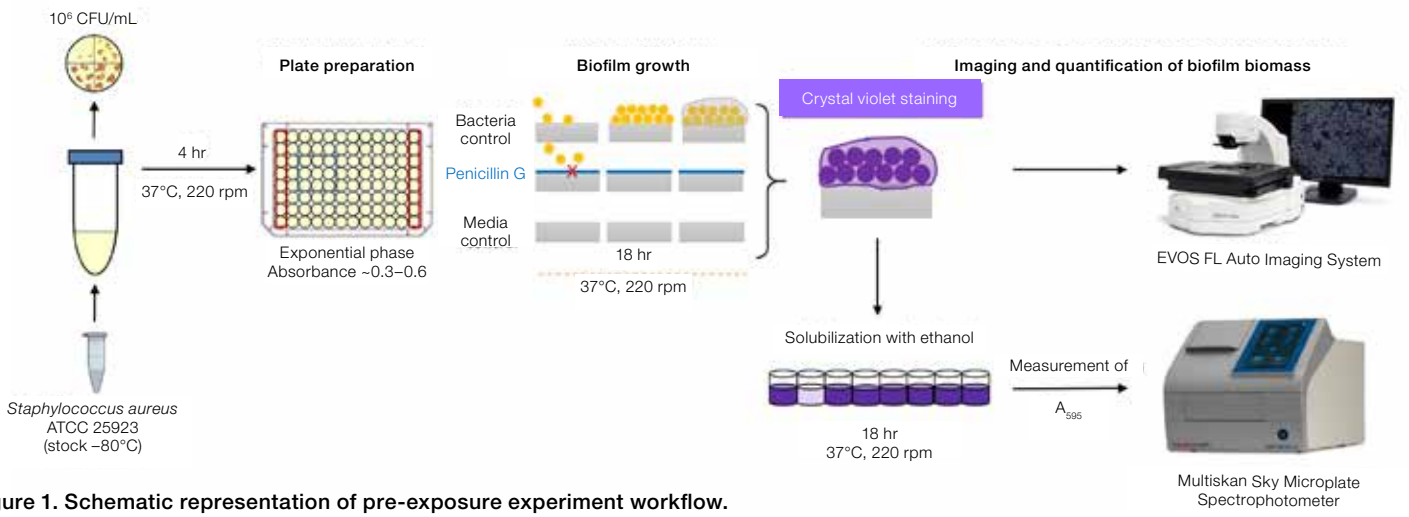

Figure 1. Schematic representation of pre-exposure experiment workflow.

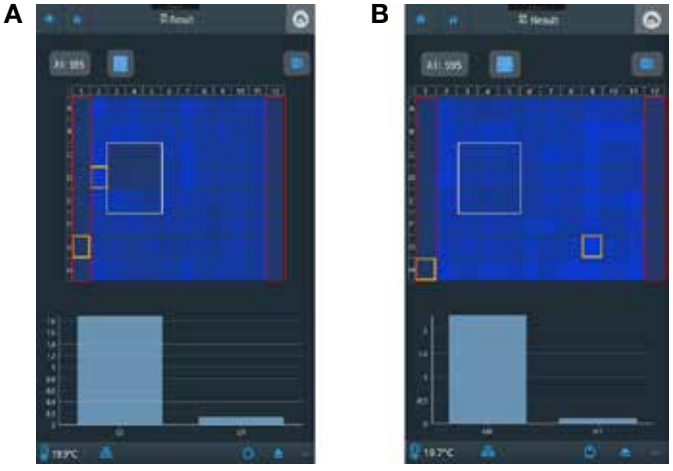

Figure 2. Heat maps generated by the Multiskan Sky Microplate Spectrophotometer after performing the endpoint measurement with crystal violet staining at 595 nm. Heat maps are from the **(A)** pre-exposure and **(B)** post-exposure assays. Red squares highlight the values corresponding to the media control; white squares highlight the values corresponding to penicillin treatment (0.1 µM, 0.05 µM, and 0.025 µM in columns 3, 4, and 5, respectively). Yellow squares highlight the maximum and minimum values, represented below the heat map in the bar graph. Wells without squares correspond to untreated biofilm controls.

Results of the pre-exposure assay are presented in Figure 3. The low absorbance values of crystal violet staining quantified in the media controls (Figure 3A) indicate an insignificant amount of biofilm biomass in those wells, as confirmed by the clean (poorly stained) brightfield images (Figure 3B). In contrast, the images captured of the young *S. aureus* biofilms (Figure 3C) formed after 18 hr show a uniformly distributed biofilm with hardly any clear spaces, corresponding to an average crystal violet absorbance of 1.213 ±0.230 (Figure 3A). In this pre-exposure assay, treatment with 0.025 µM of penicillin was found to be sub-inhibitory, with crystal violet absorbance readings (1.220 ±0.316) that were not statistically different from those of the untreated biofilms (Figure 3A). However, increasing the penicillin concentration in the planktonic *S. aureus* resulted in significantly lower crystal violet absorbance values (0.257 ±0.048 and 0.143 ±0.010 for 0.05 and 0.1 µM of penicillin, respectively). Such reduction on the biofilm biomass was further confirmed with imaging—a dramatic decrease in the number of stained cells was seen as the penicillin concentrations increased (Figures 3D–F). Of note, it can be appreciated that stained biofilms formed on the wells treated with the lowest concentration of penicillin (0.025 µM, Figure 3D) share an attachment pattern and spatial organization similar to that of the untreated controls. Images also reveal that biofilms tended to concentrate towards the edge of the wells. This is in accordance with other studies revealing that differences exist between the microbial attachment patterns across a well in a microplate [14]. Such differences in spatial distribution are caused by the amplitude of fluctuations of the shear flow that is generated when the plate is shaken in an orbital fashion. This affects not only the way the biofilm is deposited but also its morphology and survival. Such aspects need to be taken into account, since the tolerance towards antibiotics is highly affected by the biofilm morphology [15].

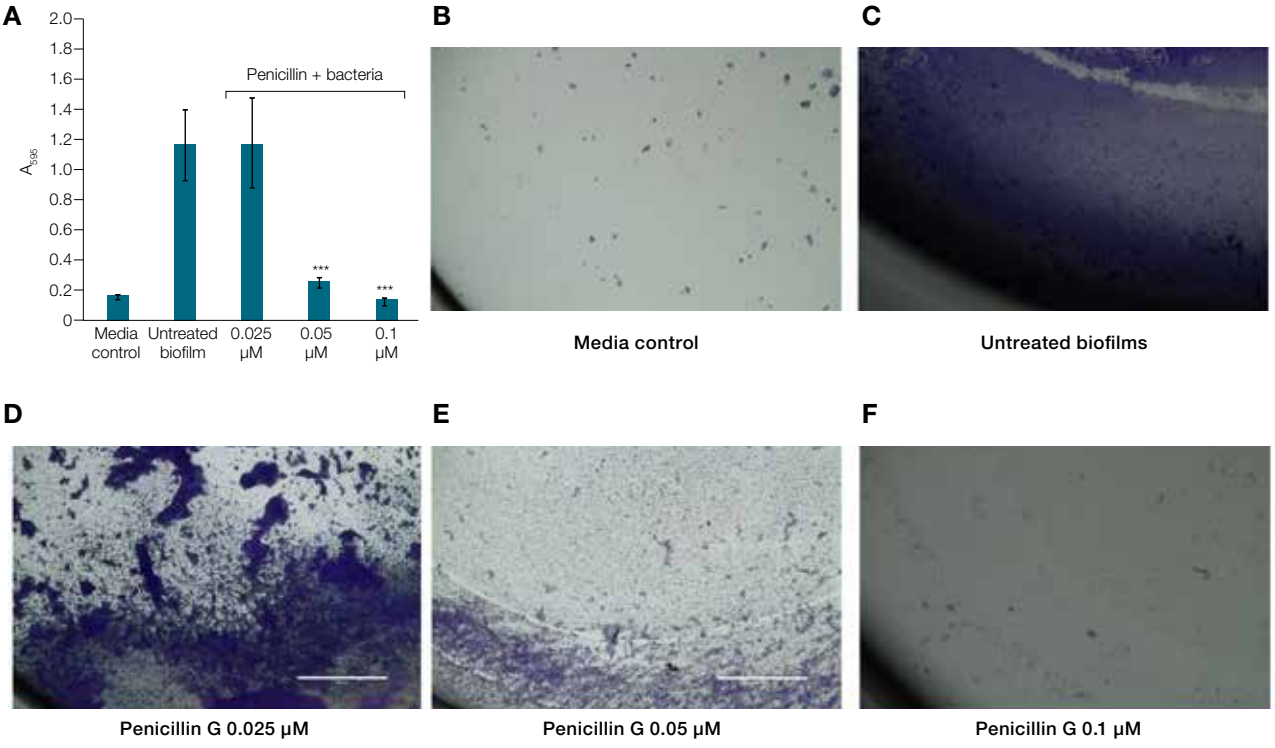

Figure 3. Quantification and imaging of crystal violet–stained *S. aureus* biofilms with and without penicillin G treatment (pre-exposure assay). (A) Absorbance at 595 nm of crystal violet–stained biofilms. Each bar represents the average of at least 3 technical replicates, with standard deviations (SD). All absorbance values were measured using the Multiskan Sky Microplate Spectrophotometer. Statistical comparisons between each treatment and the untreated biofilms were performed using an unpaired t-test with Welch's correction (*** $P < 0.0001$). **(B–F)** Representative well images of crystal violet–stained biofilms obtained under the different exposure conditions shown in (A). Images were captured using the EVOS FL Auto Imaging System (10x objective).

In the post-exposure assay, penicillin was added to preformed biofilms (Figure 4). Once developed, biofilms are characterized by high levels of antibiotic tolerance and they cannot be easily eradicated with existing antibiotics. Indeed, stained biofilms were present in samples exposed to the three different concentrations of penicillin and their distributions across the wells are very similar (Figures 4D–F). However, the microbial attachment was not as uniform when compared to the one seen in the untreated biofilms (Figure 4C). This is also supported by the measured reduction in the overall crystal violet–stained biomass of the penicillin-treated samples. Absorbance values of the penicillin-treated biofilms (1.072 ±0.101, 1.039 ±0.300, and 1.185 ±0.089 for 0.025, 0.05, and 0.1 µM of penicillin, respectively) were roughly 30% lower than the one measured for the untreated controls (1.564 ±0.289) (Figure 4A).

The pre-exposure assay (Figure 3) provides information on the ability of a compound to kill planktonic bacteria before it forms biofilms, and thus it can be attributed to biocidal activity, as in the case of penicillin G here. On the other hand, when tested on preformed *S. aureus* biofilms (Figure 4), penicillin G did not cause significant biomass inhibition, and there was not a clear concentration–response effect. In this exposure paradigm, specific anti-biofilm effects are measured and the results can be used to discriminate between broad-spectrum antibacterial agents (such as penicillin G) and specific anti-biofilm compounds, which would exert a more potent inhibitory effect on the preformed biofilms. It is important to note that crystal violet stain measures the amount of biofilm present but not the viability, so it is only useful for assessing the effects on the total biomass attached but not for evaluating the bactericidal effects [16].

The orthogonal approach used here involved the quantification of the crystal violet–stained biofilms along with brightfield imaging within a single cellular-adherence assay. Imaging and quantification can work in a confirmatory manner. In the current investigation, for instance, both methods demonstrate the inhibitory effects of penicillin G on the biofilm biomass. However, each result can also add distinctive information about the cellular event under study. This is exemplified here by the spatial distribution pattern of biofilms, which can be provided only through cellular imaging.

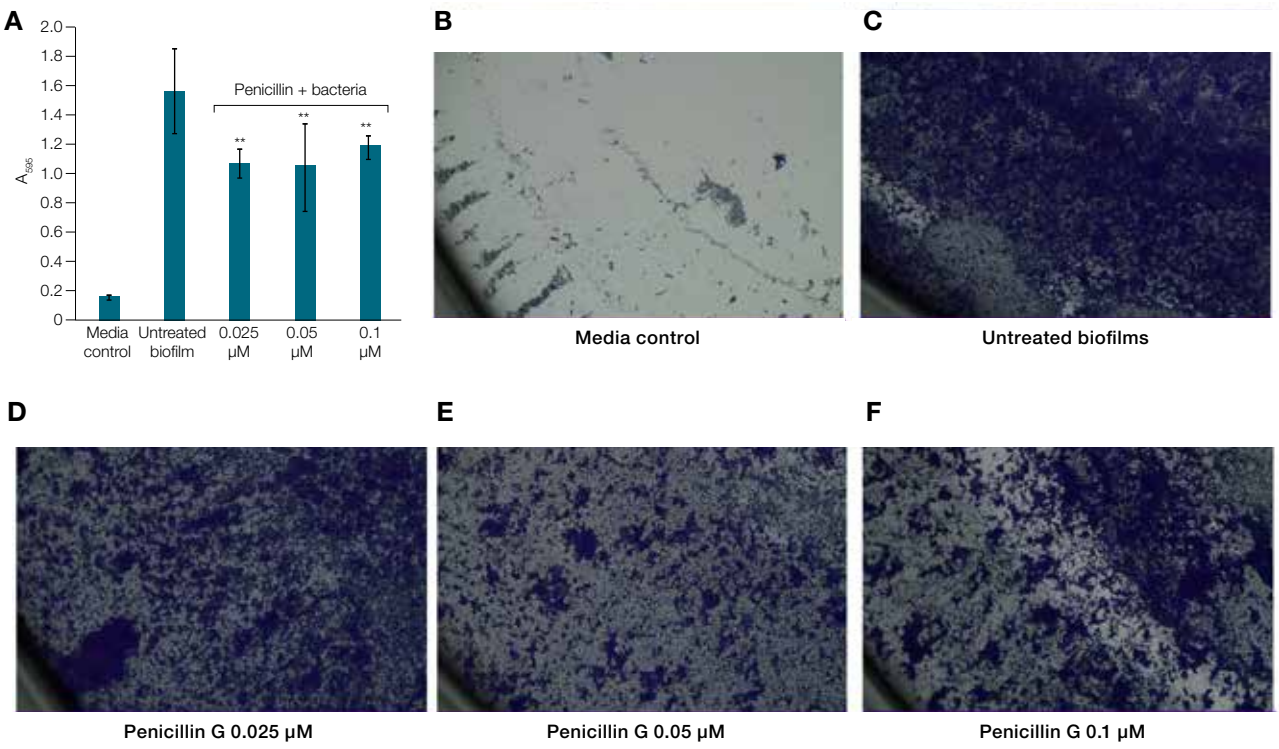

Figure 4. Quantification and imaging of crystal violet–stained *S. aureus* biofilms with and without penicillin G treatment (post-exposure assay). (A) Absorbance at 595 nm of crystal violet–stained biofilms. Each bar represents the average of at least 3 biological replicates, with standard deviations (SD). All absorbance values were measured using the Multiskan Sky Microplate Spectrophotometer. Statistical comparisons between each treatment and the untreated biofilms were performed using an unpaired t-test with Welch's correction (** $P < 0.005$). **(B–F)** Representative well images of crystal violet–stained biofilms obtained under the different exposure conditions shown in (A). Images were captured using the EVOS FL Auto Imaging System (10x objective).

thermo scientific

Conclusions

In this application note, we have shown the benefits of using orthogonal approaches for biofilms research. The workflow used here combines quantification of a photometric signal using the Multiskan Sky Microplate Spectrophotometer and brightfield imaging using the EVOS FL Auto Imaging System. By combining these results, it is possible to assess the extent to which the biofilm biomass is affected by a certain antibiotic as well as to simultaneously elucidate if any changes in the microbial attachment pattern have taken place under the tested conditions.

References

1. Donné J, Dewilde S (2015) The challenging world of biofilm physiology. *Adv Microb Physiol* 67: 235-292.
2. Skogman ME, Vuorela PM, Fallarero A (2012) Combining biofilm matrix measurements with biomass and viability assays in susceptibility assessments of antimicrobials against *Staphylococcus aureus* biofilms. *J Antibiot* 65:453-459.
3. Kruszewski KM, Nistico L, Longwell MJ et al. (2013) Reducing *Staphylococcus aureus* biofilm formation on stainless steel 316L using functionalized self-assembled monolayers. *Mater Sci Eng C-Mater Biol Appl* 33:2059-2069.
4. Guerin TF, Mondido M, McClenn B et al. (2001) Application of resazurin for estimating abundance of contaminant-degrading micro-organisms. *Lett Appl Microbiol* 32:340-345.
5. Burton E, Yakandawala N, LoVetri K et al. (2007) A microplate spectrofluorometric assay for bacterial biofilms. *J Ind Microbiol Biotechnol* 34:1-4.
6. Honraet K, Goetghebeur E, Nelis HJ (2005) Comparison of three assays for the quantification of *Candida* biomass in suspension and CDC reactor grown biofilms. *J Microbiol Methods* 63:287-295.
7. Peeters E, Nelis HJ, Coenye T (2008) Comparison of multiple methods for quantification of microbial biofilms grown in microtiter plates. *J Microbiol Methods* 72:157-165.
8. Dazzo FB, Sexton R, Jain A et al. (2017) Influence of substratum hydrophobicity on the geomicrobiology of river biofilm architecture and ecology analyzed by CMEIAS Bioimage Informatics. *Geosciences* 7:36.
9. Ming D, Wang D, Cao F et al. (2017) Kaempferol inhibits the primary attachment phase of biofilm formation in *Staphylococcus aureus*. *Front Microbiol* 8:2263.
10. Manoharan RK, Lee JH, Kim YG et al. (2017) Alizarin and chrysazin inhibit biofilm and hyphal formation by *Candida albicans*. *Front Cell Infect Microbiol* 7:447.
11. Barros J, Grenho L, Fontenente S et al. (2017) *Staphylococcus aureus* and *Escherichia coli* dual-species biofilms on nanohydroxyapatite loaded with CHX or ZnO nanoparticles. *J Biomed Mater Res* Part A 105:491-497.
12. Sandberg M, Maattanen A, Peltonen J et al. (2008) Automating a 96-well microtitre plate model for *Staphylococcus aureus* biofilms: an approach to screening of natural antimicrobial compounds. Int *J Antimicrob Agents* 32:233-240.
13. Djordjevic D, Wiedmann M, McLandsborough LA (2002) Microtiter plate assay for assessment of *Listeria monocytogenes* biofilm formation. *Appl Environ Microbiol* 68:2950-2958.
14. Salek MM, Sattari P, Martinuzzi RJ (2012) Analysis of fluid flow and wall shear stress patterns inside partially filled agitated culture well plates. *Ann Biomed Eng* 40:707-728.
15. Kostenko V, Salek MM, Sattari P et al. (2010) *Staphylococcus aureus* biofilm formation and tolerance to antibiotics in response to oscillatory shear stresses of physiological levels. *FEMS Immunol Med Microbiol* 59:421-431.
16. Pitts B, Hamilton MA, Zelver N et al. (2003) A microtiter-plate screening method for biofilm disinfection and removal. *J Microbiol Methods* 54:269-276.

Find out more at **thermofisher.com/multiskansky** and **thermofisher.com/evos**

ThermoFisher SCIENTIFIC